[American Journal of Science, Vol. 308, April, 2008, P. 399–420, DOI 10.2475/04.2008.01]

American Journal of Science

APRIL 2008

FURTHER SHRIMP GEOCHRONOLOGY ON THE EARLY CAMBRIAN OF SOUTH CHINA

W. COMPSTON*, ZICHAO ZHANG**, J. A. COOPER***, GUOGAN MA** and R.J.F. JENKINS§

ABSTRACT. Zircon $^{206}Pb/^{238}U$ ages are reported for bentonites from two Cambrian sections in South China, the Meishucun and the Fandian. The analyzed zircons vary widely in age because of the presence of detrital and altered grains. Spot ages were corrected for calibration drift during analysis, and the age of reference zircon SL13 was calibrated as 580 Ma against other standards using SIMS. Use of mixture modeling was essential to resolve the different age components and to identify the volcanic ages. Two age groups occur within the Meishucun Bed 5 bentonite, of which the larger at 518.7 ± 2.5 Ma (σ) is interpreted as a post depositional zircon growth event and the other at 539.4 ± 2.9 Ma as the volcanic age. Bentonites from the Meishucun Bed 9 and its Fandian equivalent have two age groups, 526.5 ± 1.1 Ma and 540.2 ± 1.0 Ma. We interpret the younger of these as the tuff magmatic age and the older as detrital. Small shelly fossils indicate Meischucunian Bed 5 is an equivalent of the late Nemakit Daldynian, and its 539.4 ± 2.9 Ma age both closely times the base of the Cambrian and is a maximum for the basal Tommotian. The 526.5 ± 1.1 Ma for Bed 9 and its equivalents approximates the close of the Tommotian.

INTRODUCTION

The ages of sedimentary sequences can be found by the dating of zircons from interbedded volcanic rocks, provided that detrital and altered zircons and zircon inclusions can be recognized and excluded. Bentonites occur within early Cambrian sediments of South China, one of which from the Meishucun Bed 5 was dated previously (Compston and others, 1992) using the Sensitive High Resolution Ion Microprobe (SHRIMP). This was done to clarify the age of the Precambrian/Cambrian boundary, which was then uncertain within the range 530 Ma to 570 Ma. Since the late 1980s, improvements in instrumental stability and especially in the understanding of instrumental effects on apparent $^{206}Pb/^{238}U$ ages have increased the age precision. In addition, there has been an important recent change in the use of the original reference zircon, SL13: its operational age is not 572 Ma as measured by mass spectrometric isotope dilution (MSID), but 580 Ma as calibrated using SIMS against later zircon standards (Black and others, 2003; Black and Compston, unpublished data). We therefore recalculate and revise our published age for the Bed 5 bentonite in this paper, in addition to reporting new SHRIMP ages for other bentonites from the Meishucun sequence and from one of its stratigraphic correlatives in South China.

Every volcanic sample reported here contains inherited zircons, most of which cannot be recognized before the actual age is measured. They become of serious concern when their ages are only a few percent older than the volcanism, and when

*Research School of Earth Science, The Australian National University, Canberra, ACT, 0200, Australia; william.compston@anu.edu.au

**Yichang Institute of Geology and Mineral Resources, Yichang 443003, China

***Department of Geology and Geophysics, Adelaide University, Adelaide, S.A. 5005, Australia

§South Australian Museum, Adelaide, S.A. 5000, Australia

their values might merge with the normal fluctuations in the volcanic ages that arise from analytical uncertainty. Similarly, lowered $^{206}Pb/^{238}U$ ages caused by small percentages of Pb loss might also merge with the volcanic age, so that an apparently continuous distribution of $^{206}Pb/^{238}U$ ages from above to below the volcanic age can be produced. We have addressed this problem by the use of mixture modeling (Sambridge and Compston, 1994): the collective ages from each volcanic horizon are resolved into two or more discrete groups, each having a normal distribution and a different mean, by calculating the lowest residual variance from iterative choice of age and proportions. Whether there is serious departure from normal distributions for the $^{206}Pb/^{238}U$ age populations owing to Pb loss will be examined in the text. The method also requires valid estimates for the uncertainty of each age, which we have reassessed here for all analyzed spots. Not all the data sets are well adapted for our purpose: some are too small, some have high internal uncertainty due to low counting rates (low U), and one in particular has been disturbed by unusual instrumental effects.

There is a second problem related to the presence of inherited zircons, which is shared by all zircon-dating methods. Suppose a single well-defined age group that is wholly inherited dominates the zircon concentrate while the zircons that crystallized from the tuff are very minor in abundance. How can the tuff zircons be recognized? The problem can be solved if accurate $^{207}Pb/^{206}Pb$ measurements are available using MSID, on the principle that the youngest concordant zircon age could belong to the tuff. There is the proviso of course that at least one such grain can be found, which requires that many MSID analyses must be made (for example Landing and others, 1998). In contrast, the problem is difficult to resolve using $^{206}Pb/^{238}U$ ages alone, for which a small youngest group can be interpreted as caused by Pb loss.

The Concordia diagram has not been used for the presentation of the final ages, because SHRIMP cannot measure $^{207}Pb/^{206}Pb$ with enough precision per spot to be useful in samples as young as Palaeozoic. Display of the spot-ages for standard and sample is given instead as plots of $^{206}Pb/^{238}U$ age against time of analysis within each session. We attempt to compensate for the imprecise $^{207}Pb/^{206}Pb$ measurement per single spot by assessing the $^{206}Pb/^{238}U$ ages statistically *en masse* per session and per volcanic horizon. In this way we hope to draw valid conclusions about different age components within the samples, and to see how far this approach can usefully resolve the ages of different tuff horizons in the early Palaeozoic.

The present paper represents a third revision of the original data of Compston and others (1992) for the age of the Meishucun Bed 5 bentonite. The first resulted from the application of mixture modeling to the published data, which were found to be better fitted by two age components instead of one: the undisturbed age was revised to 530 Ma. Jenkins and others (2002) published a second revision using a different data-assessment paradigm to process the original primary data and that for another sample of the same Bed 5 bentonite. They calibrated the age for SL13 using SHRIMP as 580 Ma relative to 1850 Ma for the QGNG zircon standard, not 572 Ma as directly measured using MSID, and called on fine scale Pb loss within SL13 to account for the difference. Black and others (2003) showed that fine scale Pb loss within SL13 is very unlikely and proposed instead the operation of a 'matrix' effect peculiar to SL13 that increased its measured age. Because both explanations for the SL13 effect give 580 Ma for its operational age, the previous ages of the Bed 5 samples in Jenkins and others (2002) are very similar to those in the present paper, which has become the third revision. There is also a difference in the uncertainties calculated per spot age, which is relevant to the results from mixture modeling. Both use the internal uncertainty per spot augmented by that of the standard, but the present paper also includes the uncertainty from the calibration drift per spot with the internal uncertainty.

All uncertainties in age are one standard deviation. The primary and reduced data are available on request from the first author.

THE SAMPLES

Ma Guogang and Zhang Zichao collected the first five samples below from two early Cambrian sections in South China, the Meishucun Section and the Fandian Section. The two latter and the sample locations are shown in figure 1. J. A. Cooper and Yin Jicheng from the Chengdu College of Geology collected sample MDP-1. Compston and others (1992) reported SHRIMP analyses for YMB-1, which were reassessed by Jenkins and others (2002). Here we again reassess the original data, and we report SHRIMP analyses of samples W-1, WX-1, WL-2 and MDP-1 made at intervals between the early 1990s and the early 2000s.

YMB-1 is the original volcanic dated by Compston and others, 1992, an altered bentonite layer within Bed 5 of the Meishucun Section. Bed 5 consists of crystal debris-bearing mica-clay, with abundant shelly fossils that belong to the *Anabarites-protohertzina* Zone (see Steiner and others, 2007). The grain mounts are Z837 and Z903. The White Clay horizon is a second Bed 5 sample, placed on grain mount Z1367.

W1 is a thin bentonite layer within tuffaceous marl at the base of the Meishucun Bed 9, East Yunnan (fig. 2), just above the disconformity plane between the Dahai Member of the Zhujiaquing Fm, Bed 8, and the base of the Shiyantou Formation, Bed 9. Bed 8 belongs to the *Watsonella crosbyi* Zone (Steiner and others, 2007) and bed 9 to a succeeding poorly fossiliferous interzone believed to overlap the ?later Tommotian. Zircon grain-mounts are Z1297 and Z1457.

WX-1, mount Z1442, is from crystal-vitric tuffaceous dolomite at the base of the 'Xiaowaitoushan' Member of the 'Yuhucun' Fm, or its equivalent, the Daibu Member of the Zhujiaquing Formation (see Steiner and others, 2007). Qian and Bengtson (1988) found this interval to be unfossiliferous and indicated it to represent part of the Sinian.

WL-2 is a debris-tuff from the base of the Cambrian Jiulaodong Fm, which outcrops in the Fandian Section of the Leshan area, south Sichuan. Based on comparisons of shelly fossils, and its homotaxial placement, the stratigraphic level of sample WL-2 approximates that of sample W1.

MDP-1 is a second sample of the Jiulaodong Fm, a thin tuff band from Maidiping, some 25 km from the Fandian Section. It has a similar stratigraphic level to that of WL-2 from the Fandian Section.

ANALYTICAL PROCEDURES

The separated zircons were analyzed as sectioned in polished, gold-coated grain mounts, which were repolished to expose new zircon surfaces and rerun as denoted by the sessional dates. The SL13 standard alone was used. Analytical sessions used the routine nine mass-channels for zircon dating, and common Pb was estimated by the $^{208}Pb/^{206}Pb$ method for SL13 and the $^{207}Pb/^{206}Pb$ method for the sample zircons (Compston and others, 1984). The reproducibility and internal uncertainty in age per spot for the SL13 zircon are performance indicators for each session. The internal uncertainty is controlled primarily by ion counting statistics, which depends in turn upon the size of the primary $^{16}O_2^-$ beam. Half of the sessions reported here have SL13 age uncertainties per spot between 1.3 percent and 1.9 percent, and the rest range between 0.9 percent and 0.7 percent. The uncertainties for the means of the SL13 ages per session are lower still at about 0.4 percent.

Black and others (2003) propose that unrecognized instrumental effects may dominate the spread in apparent $^{206}Pb/^{238}U$ age per session for SL13, rather than variable Pb loss within the crystal: they raise the possible presence of drift and/or sharp changes in the age calibration during the session. For data sets in which ion-counting

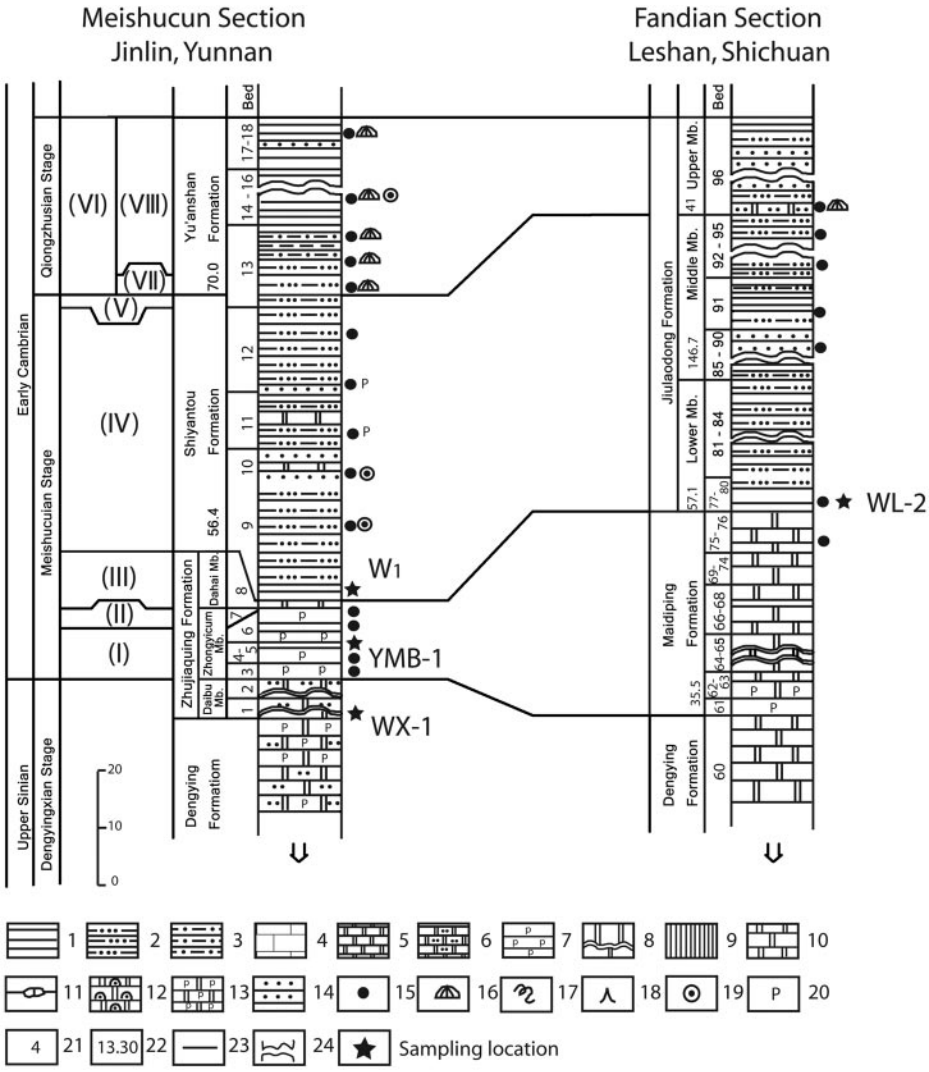

Fig. 1. Relative stratigraphic positions of the analyzed volcanics. 1) Shale; 2) argillaceous dolomite; 3) sandy dolomite; 4) limestone; 5) dolomite; 6) argillaceous siltstone; 7) phosphorite; 8) chert-banded dolomite; 9) silicolite; 10) Clastic dolomite; 11) lime lenticles; 12) bird's eye dolomite; 13) phosphorus-bearing dolomite; 14) silty; 15) fossil location; 16) trilobite; 17) trace fossils; 18) sponge fauna; 19) microflora; 20) shelly fossils; 21) bed number; 22) stratigraphic thickness; 23) chrono-correlation; 24) abbreviated symbol of stratigraphic thickness. Small shelly fossil zonation after Steiner and others (2007): (I) *Anabarites-Protohertzina* Assemblage Zone; (II) Bed 7 equivalent of *Paraglobrilus subglobosus-Purella squambulosa* Assemblage Zone; (III) Bed 8, *Watsonella crosbyi* Assemblage Zone; (IV) Poorly fossiliferous interzone above, Bed 8; (V) *Sinosachites flabelliformis-Tannuolina zhangwentangi* Assemblage Zone ; (VI) *Pelagiella subtriangulata* Taxon Range Zone (VII) *Parabadiella* Zone (yielding early trilobites); (VIII) *Wutanaspis-Eoredlichia* Interval Zone (trilobites).

noise fail to account for the observed dispersion in SL13, this idea has been extended to identify and correct for time-related drift in age. Ages are first calculated for each session as if no variation in calibration was present, a 'lowess' curve (Chambers and others, 1983) fitted to the SL13 ages plotted against time of analysis, then the fractional

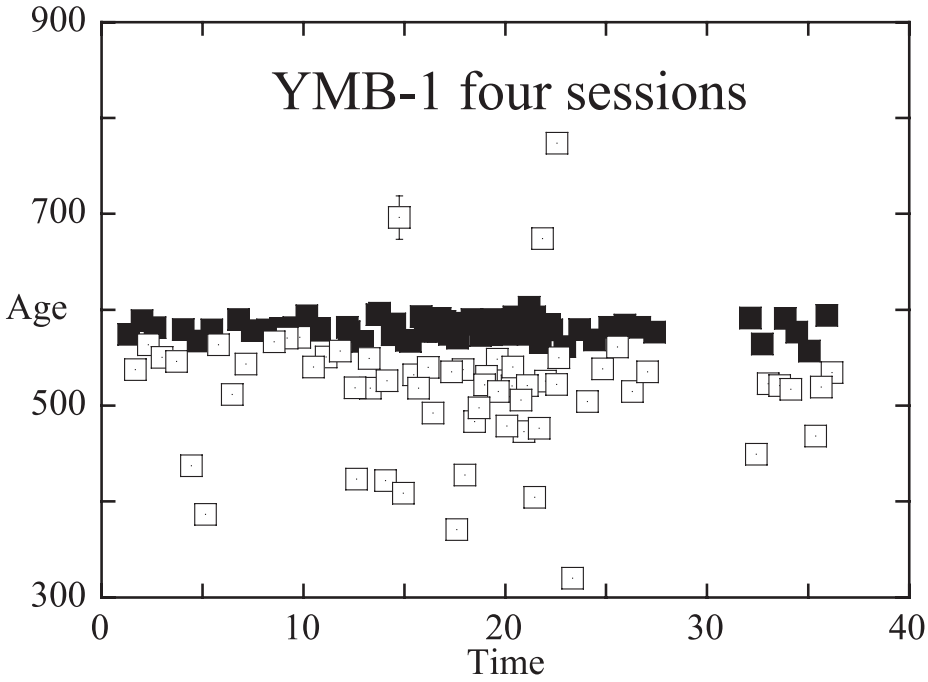

Fig. 2. Corrected SL13 and sample ages plotted against time of analysis for selected Z837, Z903 and Z1367 sessions. The black squares are SL13. The uncertainty per spot is mostly within the symbol size.

deviations from a fixed age for SL13 calculated as a function of time. The latter are then used to correct the sample ages at their particular times of measurement. Uncertainties in the lowess curve are calculated using a statistical bootstrap method and added to the ion counting uncertainties. Using this procedure, the variance of the corrected SL13 ages per session is usually fully accountable by the total measurement uncertainties. Black and Compston (in preparation) give more details and an example of calibration drift.

Black and others (2003) propose also that a sputtering effect peculiar to SL13 elevates its apparent age to about 580 Ma as recorded by secondary ion mass spectrometry, in contrast with its age of 572 Ma as measured by MSID. This was based on calibration of SL13 against the TEMORA and QGNG standards, which we have confirmed using more comparisons with TEMORA. We have adopted an operational age of 580 Ma for SL13.

We have used the kerned probability density plot (Silverman, 1986) combined with a histogram of the individual ages to display the final reduced values. The probability plot allows ages that have different uncertainties to be combined graphically, and indicates the relative frequency in age values by their summed probabilities. The different uncertainties in age arise in several ways but mainly from the potentially wide range of radiogenic Pb in zircons, which generates different ion counting rates for individual spots. They also arise from different uncertainties in the age calibration between the various sessions, by which all ages from one session can be more precise than those from a second less stable session on the same grain-mount. By contrast, the histogram plot is totally independent of the individual age uncertainties and it shows the relative frequencies of the various ages more directly by the clustering of values.

The final arbiter for enumerating significant groups of ages is mixture modeling as described above, the results of which are included in the probability density plots.

RESULTS AND INTERPRETATION

Sample YMB-1, Bed 5, Meishucun

Three analytical sessions were run for Z837 and two for Z903. One session was run later on zircons from the Bed 5 'White Clay', Z1367. Compston and others (1992) give $^{206}Pb/^{238}U$ ages for these sessions based on 572 Ma for SL13, with no correction for calibration drift, and with excess dispersion in the SL13 ages attributed only to variable Pb loss. The procedure for data assessment here is conceptually quite different. Not all of the above sessions are equally informative, some having too few sample analyses and some having high spot uncertainties. It is necessary to combine sessions to obtain an adequate sampling of the zircon populations. To illustrate the individual ages, one each of the longer Z837 and Z903 sessions and the single Z1367 session is shown combined in figure 2.

The SL13 ages in figure 2 fall on a well-fitted horizontal line and most individual deviations are accountable by internal errors. Most of the sample ages extend from a cut-off a little below the SL13 array at 580 Ma to a wide younger dispersion that indicates variable Pb loss. A few older inherited zircons are present, some (not shown) older than 650 Ma. This dispersion of zircon ages is far greater than most from volcanic rocks and indicates their extensive chemical alteration and the presence of inherited zircon.

The question is whether the dispersion contains any additional structure. To examine this, all ages for the Bed 5 zircons are plotted as their kerned probability

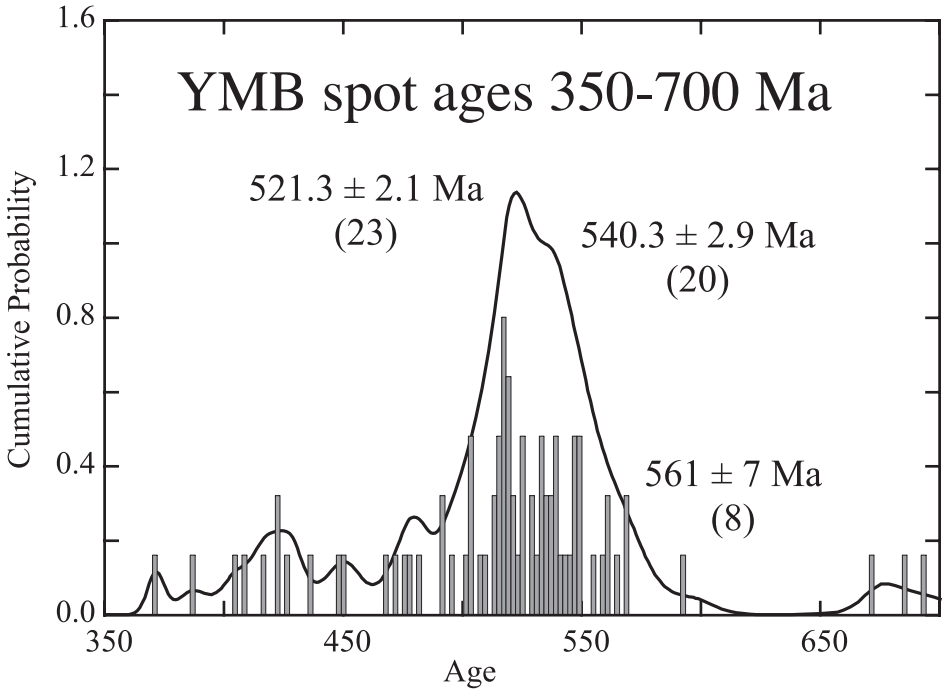

Fig. 3. Ages for combined YMB-1 sessions, shown as their kerned probability density and as a histogram. The histogram bin width in this and later plots is 2 Ma. It has been made smaller than the age uncertainties in order to display most of the individual values.

density in figure 3. Many are single spot-ages per grain, others are single values for the mean replicates per grain that have been 'screened' by testing for equality. Any significantly low value in two or more spots on a single grain was discarded and the weighted mean age for the grain was formed from the remainder. A total of 73 mean ages and single ages were combined for mixture modeling, which gives the age groups shown in figure 3. The largest modeled age group at 521 Ma is close to the peak of the probability distribution, while the 540 Ma group on the high-age side appears as a shoulder on the probability plot.

Figure 4 is another probability plot using the same data that have been truncated by rejecting age values below 480 Ma, which we consider a younger limit for imprecise spot-ages that might be plausible estimators of early Cambrian ages. The probability peaks have similar values to those shown in figure 3 but now correspond more clearly with the histogram and the remodeled age groups. The young ages that were rejected by screening evidently made little contribution to the low age tails of the main groups and did not bias them perceptibly. This is an important observation, as it implies that the scattered Pb loss did not change the age distribution sufficiently to vary the modeling results. The histogram in figure 4 also clearly shows similar groups to probability density and mixture modeling.

A more sensitive way to search for significant age groups is the use of mixture modeling for each session separately, in which only the internal uncertainties of the spot ages should be used. This allows more sensitivity in the resolution of groups than the use of their larger total uncertainties. Table 1 summarizes the modeling for the six YMB 1 sessions, which we present to test the idea from the combined sessions that two age groups are dominant. Age groups older than 540 Ma (not shown in table 1) are present in two sessions but the rest are accountable mainly as 540 Ma and 518 Ma

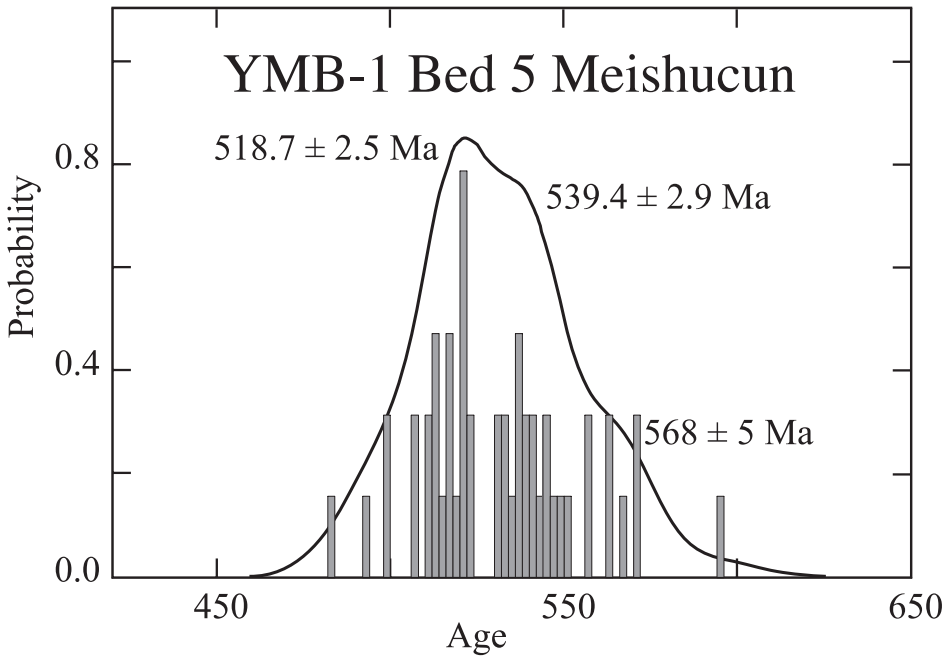

Fig. 4. Probability density for 49 ages from YMB-1 zircons between 480 Ma and 595 Ma. The age values shown are given by mixture modeling and independently match the probability peaks.

TABLE 1

Mixture modeling results for the six YMB 1 sessions

session	N_{total}	N_{540}	540 Ma group	±	N_{518}	518 Ma group	±
Z1367 28/9/92	12	3	539.6	5.0	9	520.0	2.9
Z903 12/3/91	12	5	535.2	4.3	5	517.5	4.8
Z903 16/1/90	11	5	543.5	4.2	1	512.0	9.0
Z837 16/5/90	10	0			3	521.1	5.0
Z837 25/8/90	9	2	542.9	5.6	6	515.5	2.7
Z837 01/9/89	5	1	535.5	4.9	2	521.6	3.3
weighted mean			539.2	2.1		518.6	1.5

groups. Five sessions show one or more ages within error of 540 Ma. One, 16/5/90, does not, either by chance of selection for analysis, or because any 540 Ma ages fell within the uncertainties of a large older group at 550 ± 3 Ma present in this session. All sessions show younger groups within uncertainty of 518 Ma.

Because of its reproducibility, we consider that the age group at 518 Ma is real and signifies a geochemical event that was imposed on the zircons at that time.

Sample W1, Bed 9 Z1297

The 86 sample analyses for this mount show an exceptionally wide dispersion in $^{206}Pb/^{238}U$ ages towards very young values. Instrumental drift in age calibration has been found in three out of four sessions, and its successful correction is shown by the low dispersion of the SL13 ages (fig. 5). It does not much reduce the spread of the

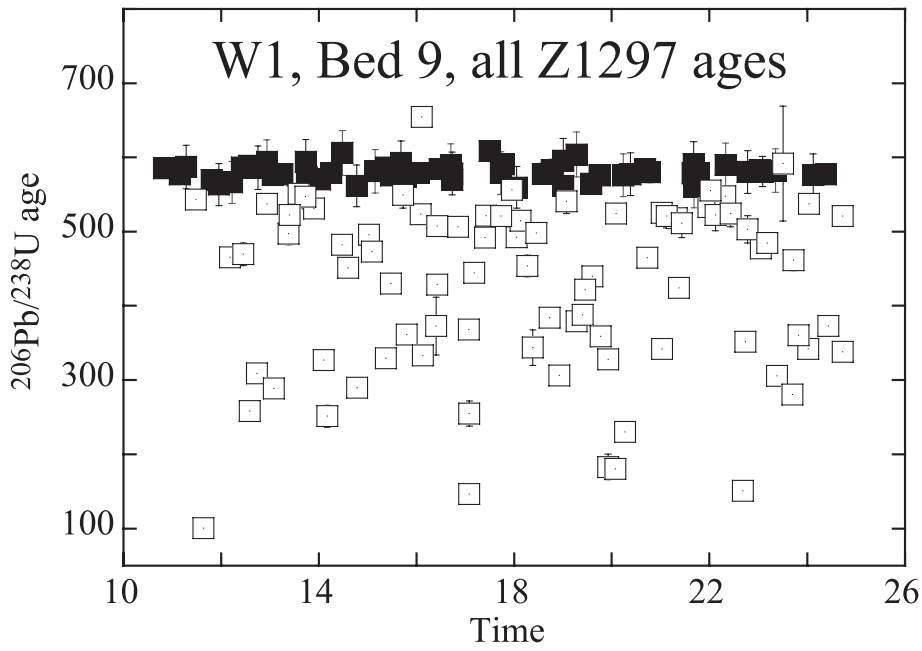

Fig. 5. Well grouped SL13 ages (black) and widely dispersed sample ages plotted against time of analysis. Data from 4 sessions on mount Z1297 are combined.

sample ages, showing that most of their dispersion is geochemical rather than instrumental. Zircon alteration is indicated also by the strong correlation of the total $^{207}Pb/^{206}Pb$ with $^{204}Pb/^{206}Pb$ for some of the sample zircons, which shows that large and variable amounts of common Pb are present in many grains. By contrast, the concentration of common Pb in the SL13 standard is much lower than the samples and constant per session to within errors. This indicates that the common Pb in these particular sample grains is not a surface contaminant but a common Pb introduced to the zircons during fluid percolation after deposition of the tuff.

Twenty-seven spot ages between 495 Ma and 560 Ma from two sessions are presented as a subset of the Z1297 data (fig. 6). The uncertainty for each age comprises the quadratic sum of their individual internal uncertainty plus the calibration uncertainty for the particular session. Both the probability density plot and mixture modeling results in figure 6 find an age group at 527 ± 3 Ma near the centre of the probability distribution, plus smaller groups at 502 ± 4 and 544 ± 4 Ma. The 527 Ma group is older than any of the younger age groups at *ca.* 519 Ma found in the Bed 5 zircon samples: is it a real age or an artifact of modeling?

The longer single sessions for Z1297 such as 4/2/92 (fig. 7) contain enough ages to be treated separately rather than combined with the other sessions. This allows use of the internal uncertainty of each age only to test the within-session uniformity in ages, which sharpens the resolution of the probability plot and of mixture modeling. Compared with the figure 6 results, both procedures give a larger oldest group at 540 ± 3 Ma and an apparently younger intermediate group at 520 ± 4 Ma, but the latter cannot be distinguished from 527 ± 3 Ma.

In contrast to this, the same intermediate age group at 527.8 ± 4.1 Ma but no 540 Ma group is given by the single 7/2/92 session (not illustrated). A less probable

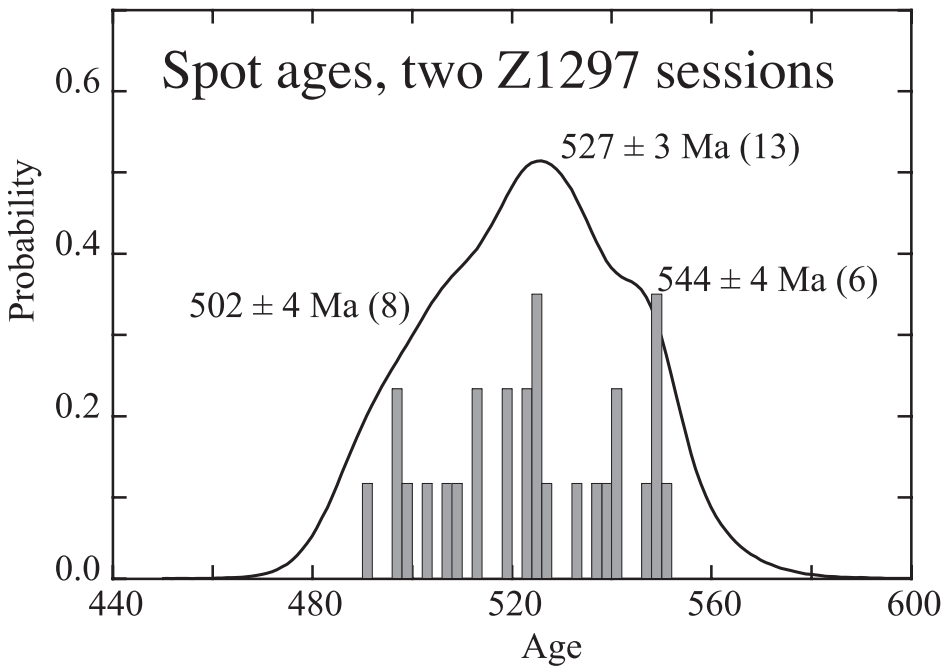

Fig. 6. Combined ages for two Z1297 sessions, sample W1, between 495 Ma and 560 Ma.

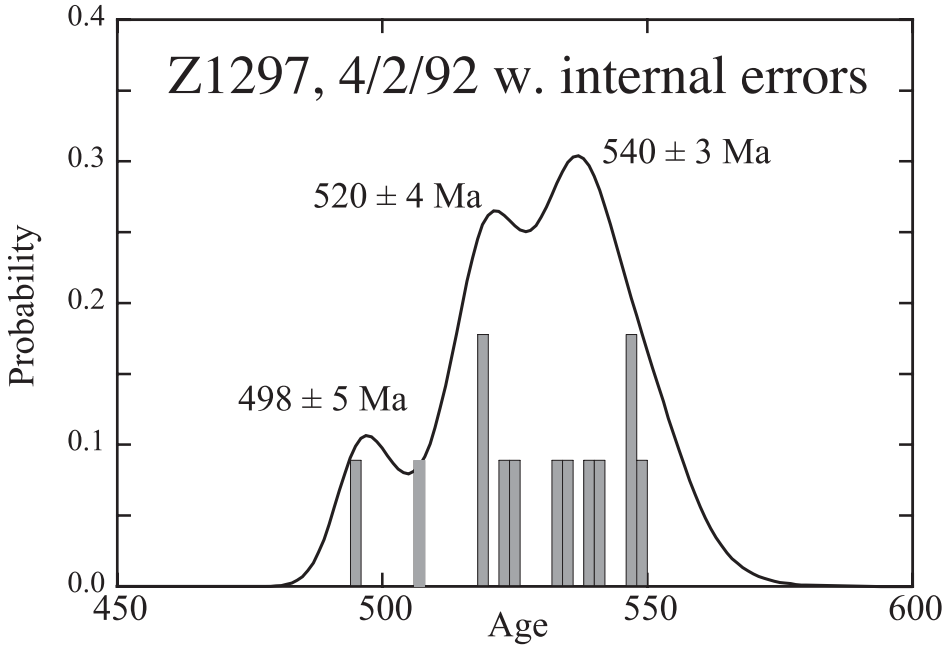

Fig. 7. Age probability density for a single W1 analytical session, 4/2/92, using internal uncertainties.

modeling solution would separate two grains at 543 ± 11 Ma and a slightly younger intermediate group at 524 ± 5 Ma.

The assessments above show that modeling can be sensitive to the numbers and precisions of the spot-ages involved, and that its conclusions need testing by dating of more samples and use of other types of evidence. The question of the existence and specific value of an intermediate age group *ca.* 527 Ma remains.

Sample W1, Bed 9 Z1457, Abraded Grains

This mount contains about twenty-five zircon grains from sample W1 that were abraded in an attempt to reduce the Pb loss found in the Z1297 mount and thereby to improve definition of the main groups. There were three initial sessions, of which only the first is acceptable with 11 sample and 9 SL13 ages. The others are too short to fit any curves with conviction, and the sample ages are too dispersed. Consequently, a later run on Z1457 was made on 8/2/07 using SHRIMP I. The combined spot-ages are shown in figure 8.

After deleting old and young extremes and including the calibration uncertainties, mixture modeling gives a main age group at 528.0 ± 2.8 Ma plus minor older and younger components (fig. 9). It does not find an age group at *ca.* 540 Ma in this sample of the W1 zircons, in contrast with the combined sessional ages from mount Z1297. It strengthens the indication of the 'intermediate' age group within the Bed 9 zircons.

Sample WX, Z1442, Upper Sinian

This is the oldest sample of the Meishucun Section, ~7.2 m below the ?lowest occurrence of shelly fossils. Consequently its age must exceed the Bed 5 age of 539 Ma, possibly by only a few million years if the Meishucun sedimentation rate remained approximately constant.

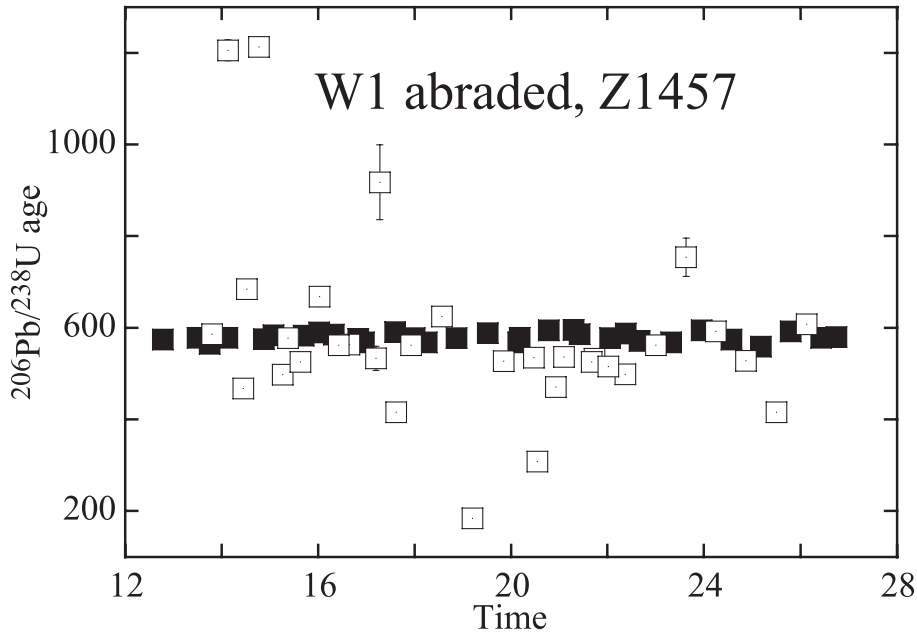

Fig. 8. Spot-ages for the 1/12/92 and 8/2/07 sessions, sample W1 mount Z1457.

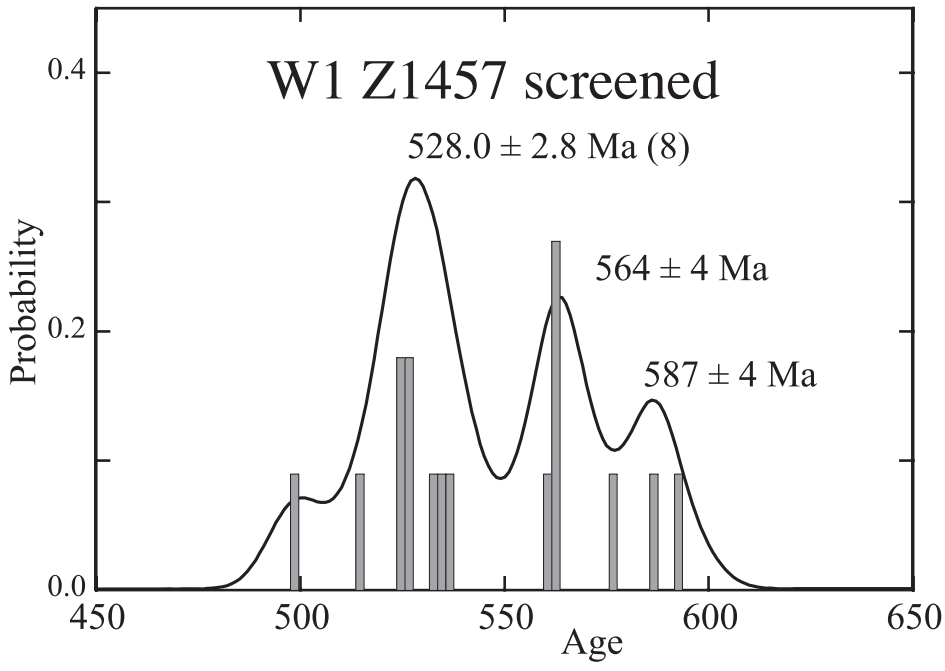

Fig. 9. Probability density and histogram for screened grain ages, sample W1, Z1457.

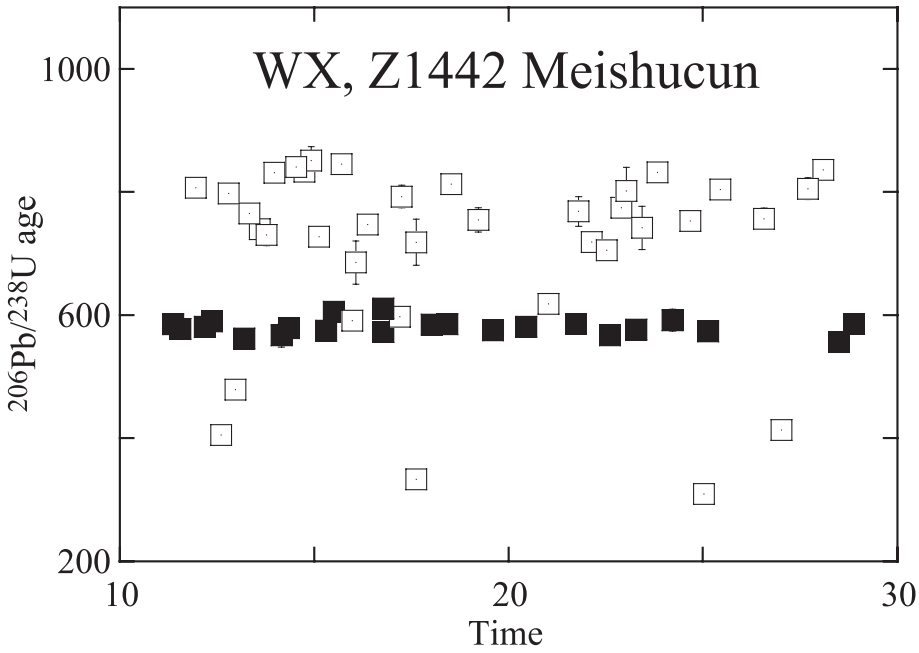

Fig. 10. $^{206}Pb/^{238}U$ ages for SL13 (filled squares) and WX samples, excluding six ages older than 1100 Ma.

Figure 10 shows the good stability of the standard, and the fact that the great majority of the sample ages exceed the age of SL13 and that of Bed 5 at Meishucun. The latter implies either that a long gap in sedimentation occurred prior to the oldest part of the Meishucun section, or that almost all the WX zircons are detrital. There is also a large dispersion in sample ages relative to analytical precision, which is consistent with Pb loss and/or inheritance. The dispersion is assessed in figure 11 using the screened ages per grain, which indicates the likelihood that three main groups are present in the scattered $^{206}Pb/^{238}U$ ages for WX.

Mixture modeling indicates three age groups: 742 ± 5 Ma, 801 ± 7 Ma and 837 ± 5 Ma, in agreement with the probability density peaks. The histogram suggests a broad 'group' of three ages at *ca.* 600 Ma, but there are only two actual analyses close to 600 Ma, and only one grain in the group might be genuinely of that age. It is the older of two analyses for which the second spot is much younger and has evidently lost Pb. Another gives a spot age of 619 ± 11 Ma but the three other analyses on the same grain range widely up to 1900 Ma, showing that the grain is highly composite in age.

Sample WL-2, Z1443, Fandian Section

This tuff is correlated on faunal evidence and homotaxial placement with Bed 9 of the Meishucun Section (fig. 1), and similar age groups should be found if the correlation is correct.

The combined spot ages for three analytical sessions are shown in figure 12. After reduction using the normal method, ages from the 11/2/92 session showed outliers that were traced to an unusual correlation of secondary ion ratios with Zr_2O^+ counts. Although the effect can be corrected approximately by normalizing the apparent ages to the same Zr_2O^+, we have elected instead not to do so but to process the data in the same way as all other sessions and to accept the consequent increase in the uncertain-

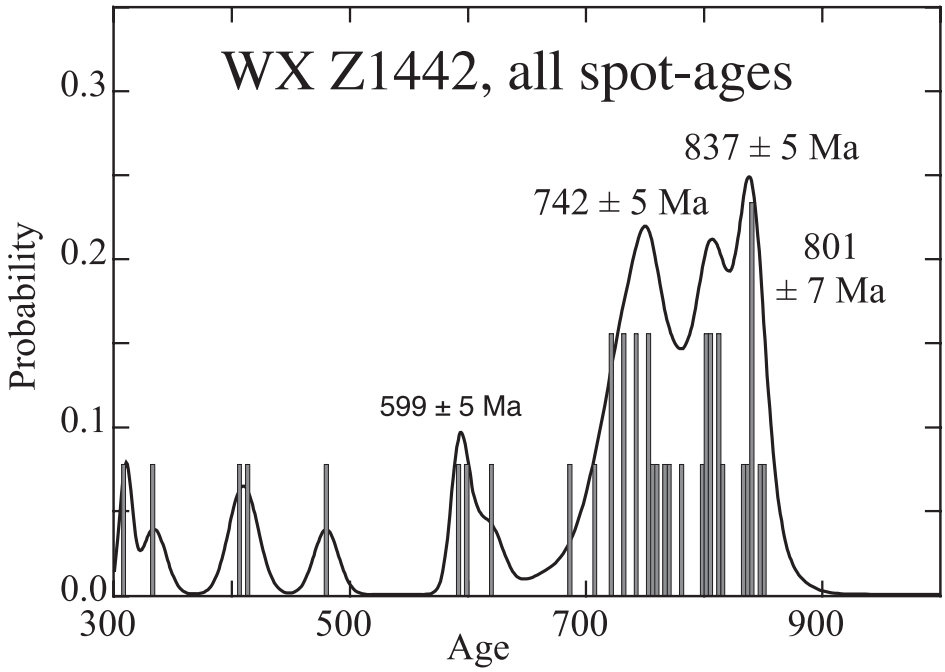

Fig. 11. Probability density, all WX zircon ages.

ties of the spot ages. Their larger uncertainties mean that the contribution of the 11/9/92 session in mixture modeling will be diminished through the normal weighting of data by their inverse variance.

The original Z1443 grain mount was rerun at higher internal precision using SHRIMP I, but the data had a further technical complication. Many UO^+/U^+ values for SL13 during the period 21 to 27 hours were lower than the sample UO^+/U^+ and accompanied by differential discrimination, probably because of proximity of the SL13 chip to a large bubble in the mount. Consequently, only SL13 data outside this time period were used for referencing the sample data.

We have combined the spot-ages between 450 Ma and 650 Ma from all three sessions, and screened out small old and young groups. Mixture modeling using the full uncertainty per age gives a large age group of 18 at 539.4 ± 1.3 Ma (fig. 13) and a nearby minor group of 4 at 528.6 ± 2.3 Ma. These two components agree with the Bed 9 pattern. There is a broad group of detrital/inherited ages at 571 Ma and older single ages up to 900 Ma.

Another assessment of the WL-2 zircons comes from the more precise rerun session alone (fig. 14), for which mixture modeling need use only the internal errors. The probability density over the range 500 to 560 Ma shows a dominant central peak at 539.2 Ma. The 539.2 Ma group is the same as in the combined WL-2 sessions in figure 13, which was resolved using the full uncertainties. It is noteworthy that two ages at *ca.* 528 Ma are still found.

Sample MDP-1, Z1205, Maidiping

This is a tuff from the lowest member of the Jiuliadong Fmn exposed in a road-cutting near Maidiping, some 25 km from the Fandian Section. It is at the same homotaxial level as WL-2 from the Fandian and W1 from the Meishucun Section. The

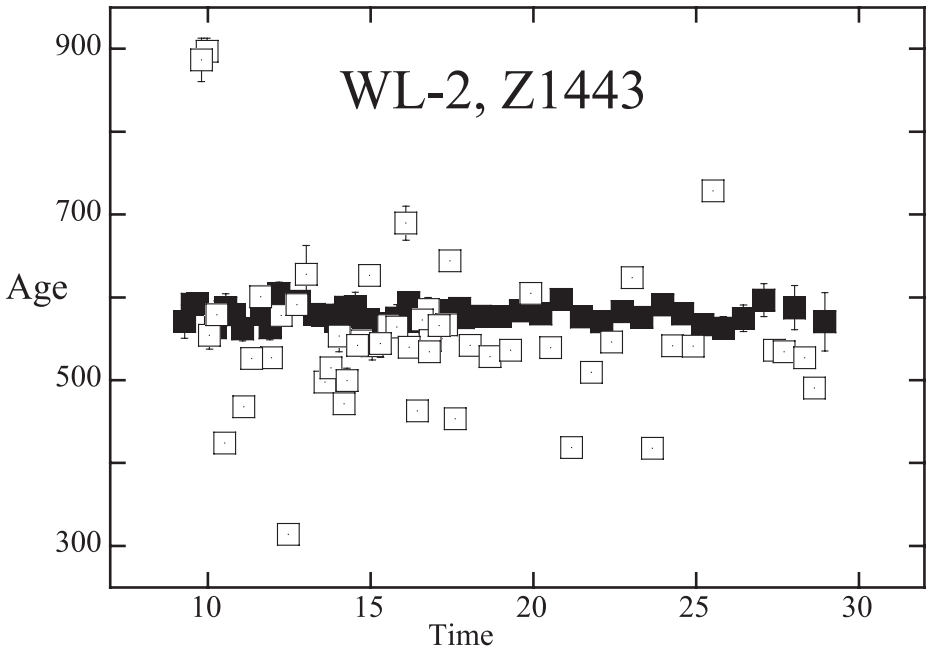

Fig. 12. Spot-ages from three WL-2 sessions, Fandian section.

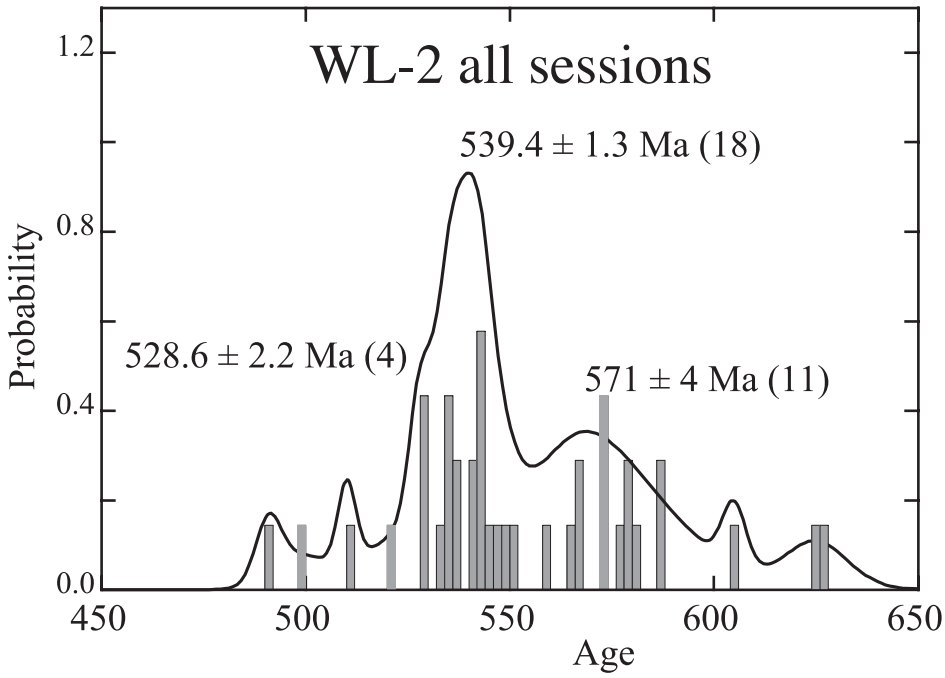

Fig. 13. Probability density plot for all WL-2 zircon ages, Fandian section.

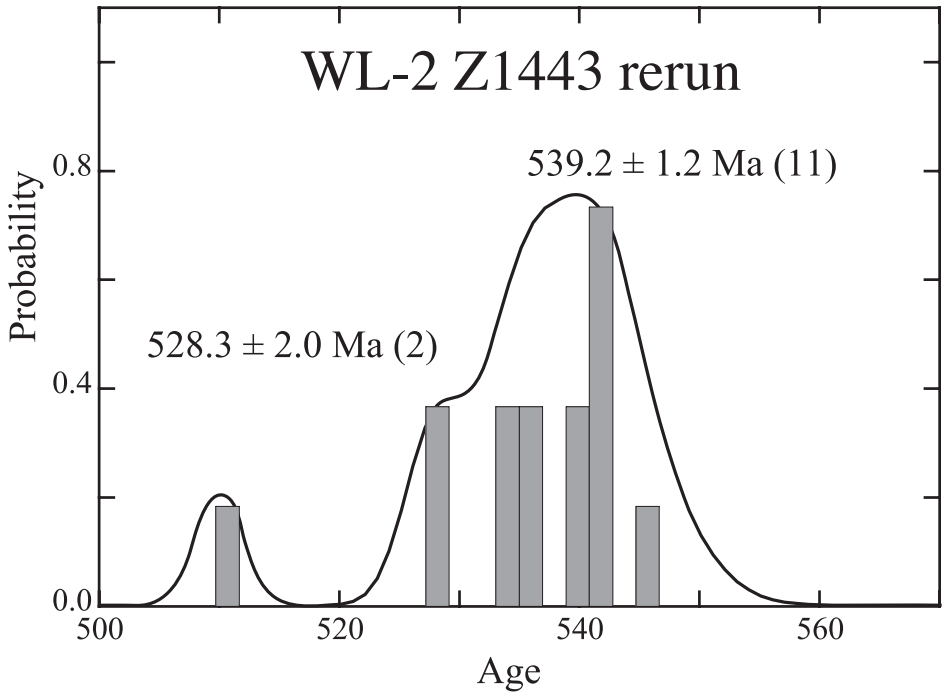

Fig. 14. Probability density plot for single session, Z1443 rerun, sample WL-2.

ages for the standard and the wide dispersion in the sample analyses are shown in figure 15, and the structure in the sample ages is shown in figure 16.

The distribution of ages is broad owing to the relatively large uncertainty per age in these sessions, but mixture modeling finds the two age components shown. The larger group, 532.3 ± 3.8 Ma, is close to the tentative 528 Ma group found in samples W1 and WL-2. It agrees with the distribution peak for WL-2 from the nearby Fandian Section, but no older component like the 540 Ma group in Z1457 is indicated by any less probable modeling solution.

In a further test for the presence of a significant age group at *ca.* 540 Ma in the MDP-1 zircons, the two MDP-1 sessions were reassessed separately using their internal uncertainty, which was approximately half the total uncertainty per age in most analyses. Modeling (table 2) found a main group at 541.3 ± 3.1 Ma (8) and one at 525.8 ± 2.4 Ma (4) for the 8/7/91 session, and 550 ± 4 Ma (4) and 527.0 ± 3.2 Ma (6) for 11/7/91. The important result here is the clear modeling of the *ca.* 526 Ma group in each session, in agreement with modeling the combined sessions.

INTERPRETATION OF ZIRCON AGE GROUPS

We return to the problem outlined at the beginning of this paper, of identifying the tuff magmatism and separating it from the ages for inherited zircons and those for post-depositional geochemical processes.

A prominent $^{206}Pb/^{238}U$ age group at c. 540 Ma has been found in all Meishucun Bed 5 grain mounts of the YMB sample and in all but one of their individual sessions (where it was probably missed as a grain sampling effect). The 540 Ma group is separable from older grains that must be inherited, and from a younger age group at c. 520 Ma. It probably denotes the Bed 5 tuff magmatism as it agrees with more recent age

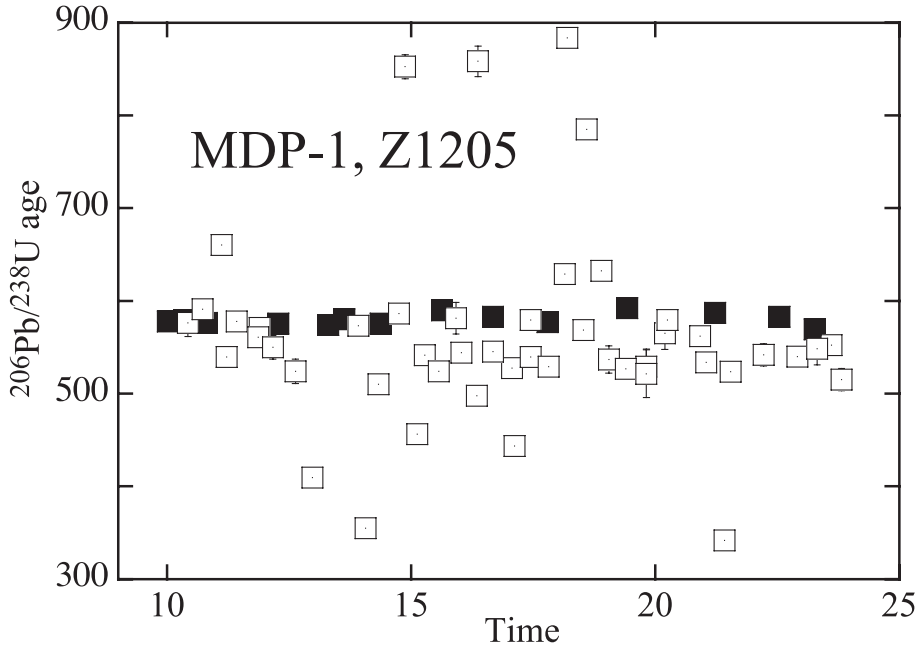

Fig. 15. Ages for two combined sessions for sample MDP-1, Z1205 8/7/91 and 11/7/91, Jiulaodong Fm. One age at 2500 Ma is not shown.

estimates elsewhere of the oldest Cambrian, and because the 520 Ma group is probably the result of a later geochemical event, on the grounds that raster-imaging using the ion probe shows that many zircons in the YMB sample have thin overgrowths of high-Th zircon.

Interpretations of ages for the Meishucun Bed 9 and its stratigraphic equivalents are less definite. The 540 Ma age was detected in all mounts and sessions from these levels except in mount Z1457, for which it can be supposed again that they were missed by sampling fluctuations. What is different about the Bed 9 level is the occurrence of an intermediate group at 526.5 ± 1.1 Ma 1 (weighted mean of two group means in table 3) that is significantly older than the intermediate group in Bed 5 at 518.6 ± 1.5 Ma. This fact raises the possibility that 526.5 Ma might be the age of tuff magmatism in Bed 9 and not a superposed geochemical event as in Bed 5, and that the 540 Ma zircons in Bed 9 are detrital not magmatic as in Bed 5. Detrital grains of 540 Ma age would be expected in Bed 9 from their presence in the underlying Bed 5.

Further speculation on these possibilities is given below in a discussion of faunal evidence for global correlations in the Early Cambrian.

BIOSTRATIGRAPHIC PLACEMENT

Recognition of the 'oldest' beds of Cambrian aspect bearing either trace fossils or mineralized skeletal parts of 'metazoans' and the chronological ranking of such strata has been subject to decades of controversy, principally because of biotic endemicity and presumed facies-related diachronic appearance of index taxa (for example Qian and Bentson, 1989; Kouchinsky and others, 2001). Khomatovsky and Karlova (1993) found that the oldest Meishucunian stage recognized on small shelly fossils, the *Circotheca-Anabarites-Protohetzina* association (now the *Anabarites-Protohetzina* Assemblage Zone of Steiner and others, 2007), shows many genera and even species in

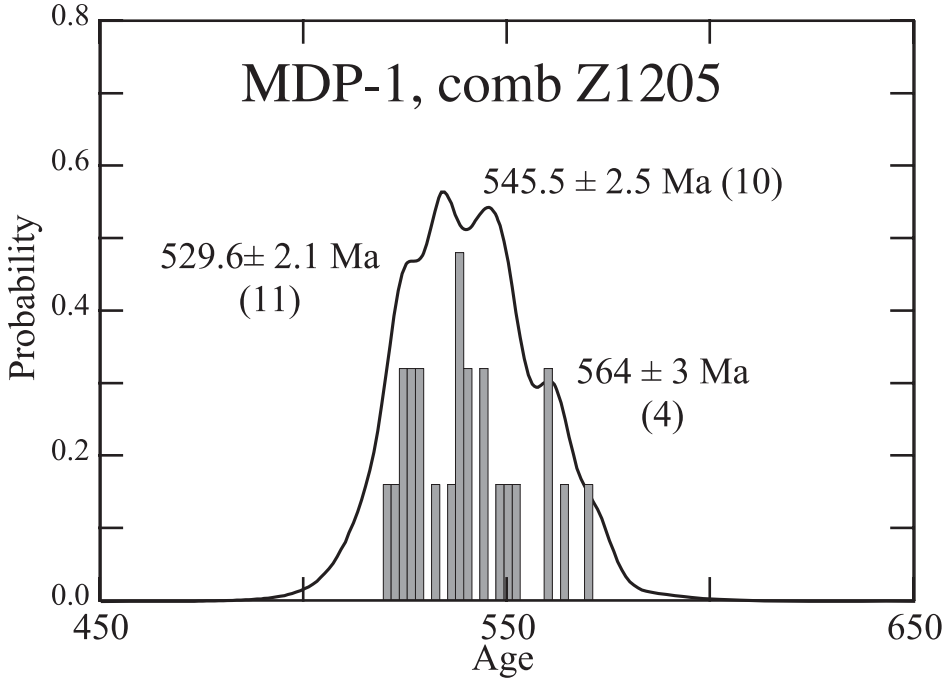

Fig. 16. Probability density for combined MDP-1 sessions.

common with the Nemakit Daldynian Stage of Siberia. Khomentovsky and Karlova (1993) further equate Bed 7 of the Zhongyicun Member and Bed 8, the Dahai Member, with the oldest Tommotian *Aldanocyathus* (= *Nochorocyathus*) *sunnaginicus* Zone. The occurrence of the arthropod trace fossils *Rusophycus* and *Cruziana* in Bed 7 (Jiang and others, 1984) is consistent with their not being older than the *Rusophycus avalonensis* Zone in the stratotypic Early Cambrian on the Avalon Peninsula, Newfoundland (for example see Narbonne and Myrow, 1988). Jiang (1984) equated the base of Bed 9 of the Shiyantou Formation, directly succeeding the Zhujiaquing Fomation (Dahai Member), with the *Dokidocyathus regularis* Zone of Siberia. Latest Atdabanian trilobites occur close to the base of the Qionzhusian Stage (Paterson and Brock, 2007).

Jenkins and others (2002) further reviewed the question of the possible correlation of the Meishucunian of southern China and classical Early Cambrian stages on various sections located on the Siberian platform, based principally on the work of Khomentovsky and Gibisher (1996), who recorded the sequential occurrence of small

Table 2

Summary of modeling results for ages of the Fandian section tuffs and MDP-1, at equivalent homotaxial levels to W1.

session	N_{total}	N_{540}	540 Ma gp	±	N_{int}	Age, int. gp	±
WL-2 rerun	13	11	539.2	1.2	2	528.3	2.0
MDP-1 8.7.91	15	8	541.3	3.1	4	525.8	2.4
MDP-1 11.7.91	12	4	(550.0)	4.0	6	527.0	3.2
mean			539.5	1.1		527.2	1.4

TABLE 3

Summary of modeling results for ages of the Bed 9 Meishucun section tuff, sample W1. "int" denotes the intermediate age group.

session	N_{total}	N_{540}	540 Ma gp	±	N_{int}	Age, int. gp	±
Z1297 15.10	17	1	(551.0)	10.0	2	524.0	6.0
Z1297 7.20	13	2	544.0	11.0	6	524.0	5.0
Z1297 4.20	13	7	539.0	3.0	4	520.0	4.0
Z1457 1.12	11	0			5	522.0	4.0
Z1457 31.10	21	0			5	531.4	3.3
mean			540.2	1.0		525.1	1.9

shelly fossils in a ~1400 + meter thick terminal Ediacaran / Early Cambrian succession in the Govi-Altay, Mongolia. Further considering Brasier and others (1996), and taking account of the sequential appearance of small shelly fossils at Bayan Gol, Govi-Altay, Jenkins and others (2002) indicated that the Meishucunian Bed 5 possibly equated with the later part of the *Ilsanella compressa- Anabarella plana* Zone of this section, and followed Komentovsky and Gibbisher (1996) in considering this interval referable to the Tommotian. Meishucunian Bed 8, representing the *Siphogonuchites-Paragloborilus-Heraultipegma* Zone of Jiang (1992), was equated with the *Watsonella (=Heraultipegma) crosbyi* Zone. The Salaany Gol Formation, interpreted as succeeding the *Watsonella crosbyi* Zone in the Bayan Gol Formation, includes late Atdabanian-early Botomian archaeocyaths in its unit 14 (Kruse and others, 1996).

Komentovsky and Gibbisher (1996) opined that the base of their bed 19 (*Tiksitheca licis* Zone) in the Bayan Gol Formation approximated the base of the Tommotian (= the Siberian *Nochorocyathus sunnaginicus* Zone) and that beds 24 and 25 (upper *Ilsanella compressa-Anabarella plana* Zone) correlated with the mid Tommotian Siberian *Dokidocyathus regularis* Zone, which would then be the age of the Meishucunian Bed 5. On the basis of this, Meishucunian Bed 9 is not older than mid Tommotian, and possibly late Tommotian. However, this view does not take account of the general assessment of Western observers that the base of the Tommotian is a regional unconformity and subject to appreciable condensation (for example Kouchinsky and others, 2001).

With further reference to Khomentovsky and Karlova (1993, fig. 8) and Brasier and others (1996), it is apparent that taxa in the upper Manykay Formation include forms that are still present in the *I. compressa- A plana* Zone at Bayan Gol. These are *Anabarites trisulcatus, Cabrotubulus decurvus*, *Siphogonuchites triangularis*, *Purella cristata*, *Latouchella korokovi*, *Ticksitheca*, *Spinulitheca*, *Halkeria*, the identified zone taxon *Anabarella plana*, *Loculitheca*, *Ladotheca dorsocava*, and *Paleosulcachites*. Hence, the Nemakit Daldynian may overlap at least as high as bed 23 in the Bayan Gol section. Comparing revised fossil lists for the Meischucunian given in Qian and Bergstson (1989) and Steiner and others (2007), Bed 5 is possibly not younger than lower bed 19 at Bayan Gol and unlikely to be younger than mid bed 23, indicating its probable age within the Nemakit Daldynian, or in the schemata of Khomentovsky and Karlova (1993), equivalent to the later part of the Manykay Formation, or the younger Nemakit Daldynian. Hence the age of 539.2 ± 2.1 Ma found herein for the Meischcunian Bed 5 is a probable minimum age for the younger Nemakit Daldynian, or a maximum for the base of the Tommotian. With reference to Jenkins and others (2002, fig. 12), the 539.2 ± 2.1 Ma age may closely approach the true age of the base of the Cambrian, allowing that the column for China in this figure now requires revision, and the

'Xiaowaitoushan' (revised as the uppermost Baiyanshao Member of the Dengying Formation by Qian and Bentson 1989) is unfossiliferous.

Utilizing data in Rozanov and Zhuravelev (1992), the appearance of *Mobigella* and *Zhijinites* in Bed 7 indicates it is probably no older than latest Tommotian, and may lie within the Atdabanian. Steiner and others (2007) indicate a hiatus at the base Bed 9, which lies within a poorly fossiliferous interzone approximately corresponding to the mid to late Tommotian. Thus the age group at 526.5 ± 1.1 Ma treated as denoting the tuff zircon magmatism at the base of Bed 9 is a maximum age for the ?late Tommotian or perhaps the older Atdabanian. The equivalent placements of the presently derived ages in the Govi-Altay sections involves a ca. 450m stratigraphic separation, emphasizing the marked condensation associated with the Tommotian and mid Meishucunian.

Rozanov and Zhuravelev (1992, p. 238) record fragmentary shelly remains resembling *Cloudina* in the ?Nemakit Daldynian upper Yudoma Formation on the Aldan River some 21 to 23.8m below the transgressive basal Tommotian boundary. Amthor and others (2003) report a zircon weighted mean $^{207}Pb/^{206}Pb$ age of 542.6 ± 0.3 Ma (2σ) and a U-Pb Concordia intercept age of 542.0 ± 0.3 Ma for tuffs respectively within and above a thrombolitic reef association with *Cloudina* in the Birba Formation of the Ara Group, Oman. Following Schoene and others (2006), we consider that a (screened) $^{206}Pb/^{238}U$ age of 540.3 ± 0.4 Ma should be used in place of the reported Concordia intercept value. *Namacalathus* fossils occur 35m below the lower dated tuff. Amthor and others (2003) consider that the disappearance of *Cloudina* and *Namacalathus* in the succession of thrombolitic reefal facies in the Ara Group constitutes a proxy for the Proterozoic / Cambrian boundary, signalled further by a marked negative carbonate carbon isotope excursion of -6 to - 7 permil $\delta^{13}C$ and subsequent sharp positive recovery to +2 or +3 permil.

The $^{206}Pb/^{238}U$ zircon ages of 539.0 ± 2.1 and 539.5 ± 0.6 Ma for the Spitskopf Member of the Ursis Formation in Namibia (Grotzinger and others, 1995: we use Grotzinger and others' $^{206}Pb/^{238}U$ ages for the present review rather than their $^{207}Pb/^{206}Pb$ ages, and apply a 0.25 percent reduction to the published values for spike calibration bias) are from tuffs in upper parts of the Schwarzrand Subgroup (Nama Group) of the Southern Nama sub-basin located respectively c. 160 and c. 300 m below a significant find of Ediacaran body fossil remains including the foliate forms *Swartpuntia* and *Pteridinium carolinaense*. Their 540 age succeeds the flourishing of the mineralized namaclathida (Grotzinger and others, 2000) that crowd parts of pinnacle reefs occurring in the Feldschorn Member of the mid Ursis Formation and built mainly by stromatolites. These reefs host the highest confirmed *Cloudina* in Namibia (Saylor and others, 1995). Shales in the upper Ursis Formation include a kind of 'twisted' tube or 'trace fossil' described by Jensen and Runnegar (2005) as *Streptichnites narbonnei*, and closely similar to a form occurring in the type Ediacara assemblage of the Flinders Ranges (for example Droser and others, 2005, fig. 3) recently named *Fusinia dorothea* Drosser and Gehring. Jensen and Runnegar (2005) posit that the hosting sediments for these traces are near the latest Ediacaran-Cambrian boundary, and our interpretation of the ages for the underlying tuffs suggests these sediments and traces are indeed Early Cambrian.

Isachsen and others (1994) gave a $^{207}Pb/^{206}Pb$ age zircon age of 530.7 ± 0.9 Ma [corrected following Schoene and others (2006) to 528.1 ± 0.9 Ma] for part of the *Rusophycus avalonensis* ichnofossil Zone in the Somerset Street section, Saint John, New Brunswick, and the same zone is recognized at Hanford Brook, 45 km to the northeast, where it is associated with small shelly fossils of the *Watsonella crosbyi* Zone (Avalonian). Jiang and others (1988) record the common occurrence of *Rusophycus* and *Crusiana* in Bed 7 at Meishucun, suggestive of a comparable zonal placement equivalent to part of the older Tommotian (Jenkins and others, 2002). The nearness of this age, within

TABLE 4

Summary of interpreted volcanic ages for late Precambrian/Cambrian tuffs, South China

Sample		Stratigraphic position	Age (Ma)
WL-2	debris-tuff	Jiulaodong Fmn, Fandian Section	528.3 ± 2.0
MDP-1	tuff	Maidiping, equivalent WL-2	526.2 ± 1.9
W1	bentonite	Bed 9, Meishucun Section	525.1 ± 1.9
YMB-1	bentonite	Bed 5, Meishucun Section	539.4 ± 2.9
WX-1	tuffaceous dolomite	Below Bed 1, Meishucun Section	≤ 742 ± 5

error, to our 526.5 ± 1.1 Ma for the base of Bed 9 and its homotaxial equivalents, is noteworthy.

CONCLUSIONS

The numerical ages of the several volcanic units reported here are collected together in table 4, and other conclusions are listed below.

1: The $^{206}Pb/^{238}U$ age group at 539.4 ± 2.9 Ma (table 4) denotes the Meishucun Bed 5 magmatism, not the age of a group of detrital zircons. This age agrees with the estimate of 538.2 ± 1.5 Ma from the same raw data by Jenkins and others (2002).

2: The biostratigraphic position of the Meishucun Bed 5 is probably within the younger Nemakit Daldynian.

This assignation takes account of revaluation of the placement of index taxa within Chinese successions (for example Steiner and others, 2007). If this assignment of biostratigraphic position is correct the isotopic age of the bed should be similar to estimates elsewhere for the Cambrian - Precambrian transition such as in Namibia and Oman (Grotzinger and others, 1995; Amthor and others, 2003). Comparison of the ages shows that they are the same within analytical uncertainties.

3: The bentonite W1 from the Meishucun Bed 9 might be as young as 525.1± 1.9 Ma (table 4). This age interprets the 540 Ma zircons that bed contains as detrital and the younger age group at 525 Ma as derived from the Bed 9 tuff magmatism. Alternatively, if the age group at 525 Ma formed by an internal geochemical event, the 540.3 ± 2.8 Ma would represent the tuff age (table 3).

4: The age difference between Bed 5 and Bed 9 obviously depends on the alternatives in the above conclusion: either 12.4 ± 2.3 Ma (σ) or between zero and 4.0 Ma.

5: The volcanic age of WL-2 from the Fandian Section is probably 528.3 ± 2.0 Ma according to inferences from mixture modeling, with 539.2 ± 1.2 Ma detrital grains (table 2).

Sample WL-2, the homotaxial equivalent of Bed 9, shows similar age distributions to sample W1 from the Meishucun section and similar interpretational problems. The probability density for the combined data is approximately unimodal, its center of distribution is 530.5 Ma, and the preferred age using mixture modeling is 533.1 ± 1.4 Ma plus a small younger age group. However, for a slightly less probable mixing model, age groups are indicated at 538.5 ± 3.7 Ma for 33 percent of grains and 529.5 ± 2.9 Ma. In addition, the internal ages for one single session give equal groups at 532.1 Ma and 541.3 Ma.

6: The weighted mean value for the 'intermediate' age groups in table 3, 526.5 ± 1.1 Ma, is our preferred combined estimate for the age of Bed 9 and its homotaxial equivalents. It may be either a maximum for the close of the Tommotian or an approximation for that time.

7: The oldest tuff in the Meishucun Section, immediately below Bed 1, is younger than 738 ± 5 Ma (table 4).

We consider that our sample of this tuff contains only detrital zircons, or that there is a long hiatus somewhere between the tuff and Bed 5, consistent with a disconformity between the Sinian and basal Cambrian.

8: All samples contain resolved age groups for detrital zircons varying from 540 Ma to 600 Ma, and a few much older individual ages.

The collective data illustrate that the main cause of dispersion in SHRIMP zircon ages is variation in the preservation and origin of the zircons, rather than dispersion in data arising from the SHRIMP method of dating.

9: The use of mixture modeling has been an essential part of the SHRIMP dating process for this paper, and low uncertainty for spot ages is mandatory for its effective use.

The $^{206}Pb/^{238}U$ ages reported here were obtained using SHRIMP mainly between 1989 and 1992. The individual spot ages are less precise than those given by current SHRIMP operation, and less precise still than current isotope dilution techniques for zircon dating. Nevertheless, collectively they have defined group ages within mixtures of detrital, volcanic and chemically disturbed zircons that have precision better than 0.5 percent (σ), which we have used to propose an age difference of about two percent between Bed 5 and Bed 9 of the early Cambrian in China. This hypothesis could be tested if tuff zircon separates that have fewer detrital zircons and much less Pb loss can be found.

10: The original SL13 reference zircon has acceptable uniformity, as shown by plots of its age against time of analysis for each analytical session. However there is concern about its absolute value per session, and one of us (R.J.F.J.) considers that structural domains in SL13 markedly control the mixture-modeling output ages, which will be researched in a forthcoming work.

ACKNOWLEDGMENTS

We thank Martin Whitehouse and an anonymous reviewer for constructive criticism of this paper, which we dedicate to Dunyi Liu for his sustained leadership of geochronology in China using SIMS analysis.

References

Amthor, J. E., Grotzinger, J. P., Schröder, S., Bowring, S. A., Ramezani, J., Martin, M. W., and Matter, A., 2003, Extinction of *Cloudina* and *Namacalathus* at the Precambrian-Cambrian boundary in Oman: Geology, v. 31, p. 431–434.

Black, L. P., Kamo, S. L., Williams, I. S., Mundil, R., Davis, D. W., Korsch, R. J., and Foudoulis, C., 2003, The application of SHRIMP to Phanerozoic geochronology: a critical appraisal of four zircon standards: Chemical Geology, v. 200, p. 171–188.

Brasier, M. D., Shields, G., Kuleshov, V. N., and Zhegallo, E. A., 1996, Integrated chemo-and biostratigraphic calibration of early animal evolution: Neoproterozoic-Early Cambrian of south-west Mongolia: Geological Magazine, v. 133, p. 445–485.

Chambers, J. M., Cleveland, W. S., Kleiner, B., and Tukey, P., A., 1983,Graphical Methods for Data Analysis: New York, Chapman and Hall, 395 p.

Compston, W., Williams, I. S., and Meyer, C., 1984, U-Pb geochronology of zircons from lunar breccia 73417 using a sensitive high mass resolution ion microprobe: Journal of Geophysical Research, v. 89, B525–B5324.

Compston, W., Williams, I. S., Kirschvink, J. L., Zhang Z., and Ma, G., 1992, Zircon U-Pb ages for the Early Cambrian time scale: London, Journal of the Geological Society, v. 149, p. 171–184.

Droser, M. L., Gehling, J. G., and Jensen, S. R., 2005, Ediacaran trace fossils: True and false, *in* Briggs, D. E. G., editor, Evolving Form and Function: Proceedings of a symposium honoring Adolf Seilacher for his contributions to paleontology, in celebration of his 80th birthday: New Haven, Connecticut, Yale University, Special Publication of the Peabody Museum of Natural History, p. 125–138.

Grotzinger, J. P., Bowring, S. A., Saylor, B. Z., and Kaufman, A. J., 1995, Biostratigraphic and geochronologic constraints on early animal evolution: Science, v. 270, p. 598–604.

Grotzinger, J. P., Watters, W., and Knoll, A. H., 2000, Calcified metazoans in thrombolite-stromatolite reefs of the terminal Proterozoic Nama Group, Namibia: Paleobiology, v. 26, p. 334–359.

Isachsen, C. E., Bowring, S. A., Landing, E., and Samson, S. D., 1994, New constraint on the division of Cambrian time: Geology, v. 22, p. 496–498.
Jenkins, R. J. F., Cooper, J. A., and Compston, W., 2002, Age and biostratigraphy of Early Cambrian tuffs from SE Australia and southern China: London, Journal of the Geological Society, v. 159, p. 645–648.
Jensen, S., and Runnegar, B. N., 2005, A complex trace fossil from the Spitskop Member (terminal Ediacaran -?Lower Cambrian.) of southern Namibia: Geological Magazine, v. 142, p. 561–569.
Jiang, Z., 1984, Subdivision of the small shelly fossil zones in Meishucunian section and their characteristics, *in* Lou, H., Jiang, Z., Wu, X., Song, X., Ouyang, L., Xing, Y., Liu, G., Zhang, S., and Tao, Y., editors, Sinian-Cambrian boundary stratotype section at Meishucun, Jinning, Yunnan, China: Yunnan, China, Peoples Publishing House, p. 102–110.
——— 1992, The Lower Cambrian fossil record of China, *in* Lips, J. H., and Signor, P. W., editors, Origin and early evolution of the Metazoa: New York, Plenum, p. 311–333.
Jiang, Z., Lou, H., and Zang, S. 1984, The Meischucunian trace fossil sequence, *in* Lou, H., Jiang, Z., Wu, X., Song, X., Ouyang, L., Xing, Y., Liu, G., Zhang, S., and Tao, Y., editors, Sinian-Cambrian boundary stratotype section at Meishucun, Jinning, Yunan, China: Yunnan, China, Peoples Publishing House, p. 100–112.
Khomentovsky, V. V., and Gibsher, A. S., 1996, The Neoproterozoic- Lower Cambrian in northern Govi-Altay, western Mongolia: regional setting, lithostratigraphy and biostratigraphy: Geological Magazine, v. 133, p. 371–391
Khomentovsky, V. V., and Karlova, G. A., 1993, Biostratigraphy of the Vendian-Cambrian beds and the Lower Cambrian Boundary in Siberia: Geological Magazine, v. 130, p. 29–45.
Kouchinsky, A., Bengston, S., Missarzevsky, V. V., Pechelaty, S., Torssander, P., and Val'kov, A. K., 2001, Carbon isotope stratigraphy and the problem of a pre-Tommotian stage in Siberia: Geological Magazine, v. 138, p. 387–396.
Kruse, P. D., Gandin, A., Debrenne, F., and Wood, R., 1996, Early Cambrian bioconstructions in the Zaukhan Basin of western Mongolia: Geological Magazine, v. 133, p. 429–444.
Landing, E., Bowring, S. A., Davedek, K. L., Westrop, S., Geyer, G., and Heldmaier, W., 1998, Duration of the Early Cambrian: U-Pb ages of volcanic ashes from Avalon and Gondwana: Canadian Journal of Earth Sciences, v. 35, p. 329–338.
Narbonne, G. M., and Myrow, P., 1988, Trace fossil biostratigraphy in the Precambrian-Lower Cambrian boundary Interval: New York State Museum Bulletin, v. 463, p. 72–76.
Paterson, J. R., and Brock, G. A., 2007, Early Cambrian trilobites from Angorichina, Flinders Ranges, South Australia, with a new assemblage from the Pararaia bunyerooensis Zone: Journal of Paleontology, v. 81, p. 116–142.
Qian, Y., and Bengtson, S., 1989, Palaeontology and biostratigraphy of the Early Cambrian Meischucunian Stage in Yunnan Province, South China: Fossils and Strata, v. 24, p. 1–156.
Rozanov, A. Yu., and Zhuravlev, A. Yu., 2002, The Lower Cambrian fossil record of the Soviet Union, *in* Lipps, J. H., and Signor, P. W., editors, Origin and Early Evolution of the Metazoa: New York and London, Plenum Press, p. 205–282.
Sambridge, M. S., and Compston, W., 1994, Mixture modeling of multi-component data sets with application to ion-probe zircon ages: Earth and Planetary Science Letters, v. 128, p. 373–390.
Saylor, B. Z., Grotzinger, J. P., and Germs, G. J. B., 1995, Sequence stratigraphy and sedimentology of the Neoproterozoic Kuibis and Schwarzrand Subgroups (Nama Group) southwestern Namibia: Precambrian Research, v. 73, p. 153–171.
Schoene, B., Crowley, J. L., Condon, D. J., Schmitz, M. D., and Bowring, S. A., 2006, Reassessing the uranium decay constants for geochronology using ID-TIMS U-Pb data: Geochimica et Cosmochimica Acta, v. 70, p. 426–445.
Silverman, B. W., 1986, Density Estimation for Statistics and Data Analysis: London, New York, Chapman and Hall, 175 p.
Steiner, M., Li, G., Qian, Y., Zhu, M., and Erdtmann, B. D., 2007, Neoproterozoic to Cambrian small shelly fossil assemblages and a revised biostratigraphic correlation of the Yangtze Platform (China): Palaeogeography, Palaeoclimatology, Palaeoecology, v. 254, p. 67–99.